Histol Histopathol (2015) 30: 971-985

http://www.hh.um.es

Histology and Histopathology

Cellular and Molecular Biology

Novel features of neurodegeneration in the inner retina of early diabetic rats

Anna Énzsöly[1,2], Arnold Szabó[2], Klaudia Szabó[2], Ágoston Szél[2], János Németh[1] and Ákos Lukáts[2]

[1]Department of Ophthalmology, Semmelweis University, Budapest, Hungary and [2]Department of Human Morphology and Developmental Biology, Semmelweis University, Budapest, Hungary

Summary. The literature indicates that in diabetes retinal dysfunctions related to neural retinal alterations exist prior to clinically detectable vasculopathy. In a previous report, a detailed description about the alteration of the outer retina was given, where diabetic degeneration preceded apoptotic loss of cells (Enzsöly et al., 2014). Here, we investigated the histopathology of the inner retina in early diabetes using the same specimens. We examined rat retinas with immunohistochemistry and Western blotting, 12 weeks after streptozotocin induction of diabetes. Glial reactivity was observed in all diabetic retinal specimens; however, it was not detectable all over the retina, but appeared in randomly arranged patches, with little or no glia activation in between. Similarly, immunoreactivity of parvalbumin (staining mostly AII amacrine cells) was also decreased only in some regions. We propose that these focal changes appear prior to affecting the whole retina and overt loss of cells. In contrast to these, most other markers used (calretinin, recoverin, tyrosin hydroxylase anti-Brn-3a and also calbindin in the optic part of the retina) did not show any major alterations in the intensity of immunoreactivity or in the number of stained elements. Interestingly, under diabetic conditions, the labeling pattern of PKC-α and calbindin in the ciliary retina showed a clear resemblance to the pattern described during development. This observation is in line with our previous study, reporting an increase in the number of dual cones, coexpressing two photopigments, which is another common feature with developing retinas. These data may indicate a previously uninvestigated regenerative capacity in diabetic retina.

Key words: Neurodegeneration, Diabetic retinopathy, Glial reactivity, Calcium binding proteins

Offprint requests to: Ákos Lukáts, Department of Human Morphology and Developmental Biology, Semmelweis University, Tűzoltó u. 58, H-1094, Budapest, Hungary. e mail: lukats.akos@med.semmelweis-univ.hu.

DOI: 10.14670/HH-11-602

Introduction

Diabetic retinopathy has been classically considered to be of vascular origin, clinically diagnosed by microaneurysms, ischemic areas, exudates, hemorrhages and proliferative lesions (Antonetti et al., 2012). However, a number of recent studies have shown that in diabetes neurodegenerative components are present earlier than clinically significant vasculopathy. Early neurodegeneration includes glial reactivity (Rungger-Brändle et al., 2000; Feit-Leichman et al., 2005; van Dijk et al., 2009), reduction of the thickness of retinal nuclear layers and apoptotic loss of ganglion cells (Barber et al., 1998; Martin et al., 2004; van Dijk et al., 2010). In line with these observations, functional studies carried out on animal models and also on human patients have reported abnormal electroretinograms, changes in color vision, loss of contrast sensitivity and dark adaptation, well before the onset of vascular lesions (Bearse et al., 2006; Aung et al., 2013). The underlying mechanisms may include microvascular abnormalities

(Curtis et al., 2009), direct toxic effect of hyperglycaemia, and abnormalities of the insulin homeostasis (Whitmire et al., 2011). Diabetic conditions may affect the outer (retinal pigmented epithelium and photoreceptor cells) and/or also the inner retinal layers that possibly respond differently to diabetes. Among the many differences between the outer and inner layers, blood supply should be a major factor contributing to possible differences in susceptibility to diabetes. The inner retina is supplied by branches of the central retinal artery in most mammalian species, while the photoreceptors are supplied by the capillary plexus of the choroid (Antonetti et al., 2006), through the retinal pigmented epithelial (RPE) cells. The photoreceptor population is also functionally dependent on the RPE which may be an additional factor to be considered.

In a previous report (Enzsöly et al., 2014), we conducted a thorough survey of outer retinal pathology in early streptozotocin- (STZ-) induced diabetes in the rat retina. We detected changes in outer segment morphology, cone opsin expression and RPE morphology preceding significant apoptosis, changes in retinal thickness or expectable vasculopathy. In the present report, we aim to extend the examination to the inner retinal layers.

An emerging number of studies from the past few years have been dealing with inner retina in STZ-induced diabetes using a series of cell-specific antibodies. These studies reported glial reactivity (Rungger-Brändle et al., 2000; Feit-Leichman et al., 2005; van Dijk et al., 2009) and decreased protein levels of tyrosine hydroxylase (TH) (Seki et al., 2004: Szabadfi et al., 2012) - with a significant reduction of the density of immunolabeled cells - and alterations in the staining of parvalbumin (staining mostly AII amacrine cells) (Park et al., 2008). Regarding the labeling patterns reported, they are believed to be dependent on many parameters, like the animal strains used, the technique of inducing diabetes, the duration of diabetes and type of treatment applied (Ly et al., 2011; Lai and Lo, 2013). Even relatively similar experimental setups can produce different results for certain cell types (Ng et al., 2004; Park et al., 2008).

In this report, we have thoroughly investigated inner retinal pathology in STZ-induced early diabetes in rats with 10 different antibodies. Glial reactivity and a decrease in the labeling intensity of parvalbumin labeled AII amacrine cells appeared in randomly distributed patches, before possibly affecting the whole retina. For the majority of the markers used, including TH, we failed to detect any significant change in the number of labeled cells or in the case of TH also in protein levels. These latter results indicate that at least some of the alterations described in earlier stages of diabetes may be transitory. We also detected changes in the staining pattern of PKC-α and calbindin antibodies, with a clear resemblance to what has been described in developing retinas. These results indicate that a previously uninvestigated regenerative capacity may be present in diabetes.

Material and methods

Animal handling

Experiments were carried out on albino Wistar male rats aged 12 weeks (n=14). All protocols were performed in concordance with the Association for Research in Vision and Ophthalmology statement for the Use of Animals in Ophthalmic and Vision Research, and were approved by the local ethical committee (Semmelweis University, number of approval: 22.1/2194/3/2010).

Details about the induction of diabetes, monitoring of diabetic conditions (body weights, sugar levels) were given in a previous report (Enzsöly et al., 2014). Briefly, streptozotocin (STZ, a dose of 70 mg/kg body weight, dissolved in 0.1 M sodium citrate buffer, pH 4.5) was injected intraperitoneally to induce diabetes to male rats (n=7), while control rats (n=7) were injected with an equivalent amount of sodium citrate buffer. At the time of the injection age and body weight of the animals were identical for STZ-injected and vehicle-injected animals. 24 hours after the injections blood glucose levels were recorded with a glucometer, and animals with higher than 20 mmol/l blood glucose level were considered diabetic (Rungger-Brändle and Dosso, 2003), and were enrolled in this study. 12 weeks after the induction of diabetes, at the age of 24 weeks all rats were euthanized with an overdose of intramuscular ketamine injection.

Tissue preparation

Eyes were oriented, enucleated, opened with an encircling cut at the cornea close to the ora serrata. For Western blotting, retinas were prepared from the eyecups, shock frozen in liquid nitrogen and stored at -80°C until used. For immunohistochemistry eyecups were immersed in 4% paraformaldehyde diluted in 0.1 M phosphate buffer (PB, pH 7.4), for two hours at room temperature. After extensive washing, the retinas were either detached and treated further as whole mounts, or cryoprotection (30% sucrose, diluted in PB, pH 7.4) was applied overnight, then the whole eyecups were embedded in Tissue-Tek CRYO-OCT Compound (Fisher Scientific, Leicestershire, UK). 15 μm thick vertical cryosections were cut and stored at -20°C until further processing. The oriented eyecups were sectioned vertically from the nasal to the temporal periphery. 4 sections were mounted onto each gelatin-coated slide in such a way that approximately every 20th section was mounted to the same slide. The mounting was performed in a strict order from the temporal to the nasal periphery and this procedure enabled us to evaluate the complete retina when immunostaining a few slides from a single retina with the same antibody. Also, knowing the order of mounting allows the identification of adjacent areas over the panel of different antibodies.

For cell-counting and thickness measurements, only the sections from the level of the optic nerve head were used and analyzed statistically. Therefore, counting and measuring were performed at identical regions of all retinas.

Immunohistochemistry

Immunohistochemistry was performed on sections and whole mounted retinas according to protocols previously published (Szabó et al., 2014). Briefly, in all specimens non-specific binding sites were blocked for 2 hours in 1% bovine serum albumin (BSA) diluted in 0.1 M phosphate buffered saline (PBS, pH 7.4) with 0.4% Triton X-100 (Sigma-Aldrich, St. Louis, MO, USA) added, followed by incubation with the primary antibodies (overnight at 4°C). Details of the cell-specific antibodies applied are given in Table 1. The bound primary antibodies were detected with species-specific fluorescent probes (Alexa 488 or Alexa 594 conjugates, 1:200, 2 hours, Life Technologies, Carlsbad, CA, USA). Cell nuclei were counterstained with DAPI (4,6-diamidino-2-phenylindole). Sections with the primary antibodies omitted were used as negative controls.

Image processing

Specimens were viewed with a laser scanning confocal microscope (Bio-Rad Radiance 2100 Rainbow Confocal Laser Scanning System, Carl Zeiss, Oberkochen, Germany) installed on a Nikon Eclipse E800 microscope (Nikon, Tokyo, Japan). For capturing images LaserSharp 2000 6.0 software (Carl Zeiss, Oberkochen, Germany) was used, then final images were imported into Adobe Photoshop 7.0 software (San Diego, CA, USA) and edited with respect to brightness and contrast.

Cell counting

In order to detect possible changes in the number of TH, calbindin, recoverin and parvalbumin labeled cell types, whole mounted temporal or nasal retinal halves were immunostained and flat mounted. Labeled cell types were counted manually over areas of 250x250 μm at 10 evenly distributed central retinal positions in case of calbindin, recoverin and parvalbumin. Data are shown as mean number of cells/mm^2 ± standard deviation (SD).

In case of TH all labeled cells per retinal halves were counted.

With protein kinase C-alpha (PKC-α) staining the number of amacrine and displaced amacrine cells labeled were counted on 10 μm thick vertical sections, at the level of the optic disc, on 3 different specimens in both controls and diabetic rats. All amacrine and displaced amacrine cells were counted over the retinal length of 700 μm in 6 different central locations per section (1, 2, 3 microscopic view fields superior and inferior to the optic disc, covering approximately half of the distance between the optic nerve and the ora serrata). These data are expressed as average number of cells over the retinal length of 1 mm ± SD.

Western blotting

Diabetic and control retinas were homogenized in Nonidet-P40 lysis buffer containing 150 mM NaCl, 1% NP-40, 50 mM Tris at pH 8.0 and protease inhibitor cocktail (Roche, Mannheim, Germany) and were kept on ice for 2 h. The lysates were centrifuged at 12000 rpm for 20 min at 4°C and supernatants were collected. The protein content of the supernatants was determined by the method of Bradford (Bradford, 1976) and all samples were diluted to a concentration of 1 mg/ml. The samples were then mixed 1:1 with reducing Tris-SDS buffer (Tris

Table 1. Primary antibodies used in this study.

Antigen	Source	Working concentration	Host and type	Epitope specificity or labeling pattern	Reference
glial fibrillary acidic protein (GFAP)	Sigma-Aldrich Kft., Budapest, Hungary	1:400	mouse monoclonal	Müller cells and astrocytes in retinal injuries	Lieth et al., 1998
vimentin	Millipore, Billerica, MA, USA	1:10000	mouse monoclonal	Müller cells	Schnitzer et al., 1981
recoverin	kind gift of Karl-Wilhelm Koch, University of Oldenburg, Germany	1:500	rabbit polyclonal	cone bipolar cells, rod and cone photoreceptors, few cells in GCL	McGinnis et al., 1997
protein kinase c-alpha (PKC-α)	Santa Cruz Biotechnology, Santa Cruz, CA, USA	1:200	mouse monoclonal	rod bipolar cells, few amacrine and displaced amacrine cells	Greferath et al., 1990
calbindin	Swant, Marly, Switzerland	1:200	mouse monoclonal	horizontal cells, few amacrine cells, few cells in GCL	Hamano et al., 1990; Chun et al., 1999
calretinin	Millipore, Billerica, MA, USA	1:2500	polyclonal rabbit	amacrine cells and cells in the GCL	Osborne and Larsen, 1996; Hwang et al., 2005
parvalbumin	Sigma-Aldrich Kft., Budapest, Hungary	1:300	mouse monoclonal	primarily amacrine cells, ganglion cells	Hamano et al., 1990
tyrosine hydroxylase (TH)	Millipore, Billerica, MA, USA	1:250	mouse monoclonal	dopaminergic amacrine cells	Nguyen-Legros et al., 1997
melanopsin	Affinity Bioreagents, Golden, CO, USA	1:80	rabbit polyclonal	intrinsically photosensitive ganglion cells	Hattar et al., 2002
Brn-3a	Millipore, Billerica, MA, USA	1:500	mouse monoclonal	ganglion cells	Nadal-Nicolás et al., 2009

0.5 M pH 6.8, 10% glycerol, 2% SDS, 0.00125% bromophenol blue, 0.5% 2-mercaptoethanol) and heated at 95°C for 4 min. 15 µl from each lysate was loaded onto a 10% polyacrylamide gel and separated by electrophoresis. After separation, proteins were transferred onto a nitrocellulose membrane (Amersham, GE Healthcare Biosciences, Pittsburgh, UK) in a buffer containing Tris–Glycine pH 8.3, 0.1% SDS and 20% methanol. The membrane was stripped and reprobed with different antibodies. In general, the non-specific reactions were blocked in 0.5 M PBS with Tween 0.05% (PBS-Tween) containing 5% BSA at room temperature for 2 h. The membranes were then incubated with the primary antibody diluted in PBS-Tween containing 5% BSA at 4°C overnight. The dilutions of the TH (Millipore, Billerica, MA, USA) and β-actin (Sigma-Aldrich, St. Louis, MO, USA) antibodies were 1:2000 and 1:5000, respectively. After washing in PBS-Tween the membranes were treated with species-specific peroxidase conjugated secondary antibody (Amersham, GE Healthcare Biosciences, Pittsburgh, UK) for 1 h at room temperature. The labeled protein bands were visualized by the chemiluminescence method using Luminata Forte Western HRP Substrate (Millipore, Billerica, MA, USA) and developed onto high performance chemiluminescence film (Amersham, GE Healthcare Biosciences, Pittsburgh, UK). Optical densities were measured using the ImageJ software (U.S. National Institutes of Health, Bethesda, MD, USA). The measured density value of each sample was normalized to its β-actin content by dividing it by the measured density value of β-actin of the same sample. The TH/β-actin ratios in control and STZ-treated samples were compared with each other.

Statistical analysis

Data are expressed as average ± SD. Body weight and blood glucose level data, and the number of parvalbumin-, calbindin-, recoverin-, PKC-α-positive cells and relative optical density data were analyzed using Student's t-test, performed with STATISTICA (version 11, StatSoft Inc., Tulsa, OK, USA). A p-value of less than 0.05 was considered statistically significant.

Results

Detailed data about the body weights and blood sugar levels of the STZ-treated and vehicle-treated animals were given in a previous report, focusing on outer retinal alterations (Enzsöly et al., 2014). Briefly, average body weight and blood glucose concentration values did not differ significantly in the two groups before the induction of diabetes (body weights were 383.8±12.6 g vs. 395.6±9.1 g, while blood glucose concentration values were 6.1±0.3 mmol/l vs. 5.8±0.3 mmol/l in controls and diabetic rats respectively, $p>0.05$, $n=7$). After 12 weeks, diabetic rats had a significantly lower body weight and higher blood glucose concentration than rats in the control group. Body weights were 457±29.5 g and 287.4±21.1 g in controls and diabetics respectively; blood glucose concentration values were 6.3±0.2 mmol/l in controls and higher than 25.0 mmol/l in all diabetic animals ($p<0.05$, $n=7$).

In a previous work dealing with outer retinal alterations in diabetes, using the same specimens (Enzsöly et al., 2014), we demonstrated that the thickness of the whole retina and the ONL alone was unchanged, there was no increase in the number of TUNEL positive elements in diabetes compared to controls and no loss of photoreceptor cells was detectable.

All these data clearly indicate that the retinas were inspected prior to apoptotic loss of cells, which is in agreement with the literature (Barber et al., 1998). Also, the retinas were analyzed prior to expectable vasculopathy, which in STZ-induced diabetes develops only on the long run, appearing approximately 12 months after the induction of the disease (Anderson et al., 1995).

Müller glial reactivity in diabetes (GFAP, vimentin)

Glial cells were labeled with GFAP and vimentin primary antibodies.

GFAP labeling in the control group was localized to the inner limiting membrane (Fig. 1a) and to the extreme peripheral retina, in accordance with the literature (Lieth et al., 1998). 12 weeks after the induction of diabetes, an inhomogeneous labeling pattern could be detected: regions with a labeling pattern similar to healthy controls were present (Fig. 1d), but also areas with intensive labeling of cell bodies of Müller glia cells showed up demonstrating glial reactivity (Fig. 1c). The regions of intensive labeling were distributed randomly over the retinas examined and were not confined to any specific (superior or inferior, central or peripheral) retinal region.

Vimentin is a marker for Müller glia cells (Fig. 1e). In contrast to the results of immunostaining with GFAP, vimentin expression was not upregulated in diabetes. Rather, we detected a slight decrease in vimentin expression, again confined to certain retinal regions (Fig. 1g). Not surprisingly, comparing adjacent sections from sequential series revealed that the regions of GFAP upregulation and vimentin downregulation coincided with each other.

Staining patterns of calcium binding proteins in diabetic retinas (parvalbumin, calbindin, calretinin, recoverin)

Parvalbumin is a marker primarily for AII amacrine cells with faint labeling in widefield amacrine, some bipolar and ganglion cells (Wässle et al., 1993) (Fig. 2a). In diabetic retinas most regions showed parvalbumin labeling identical to those of controls, with no detectable changes in staining intensity or morphology of the cells identified (Fig. 2c). However, smaller patches of less intensive labeling (Fig. 2d) could be revealed in almost

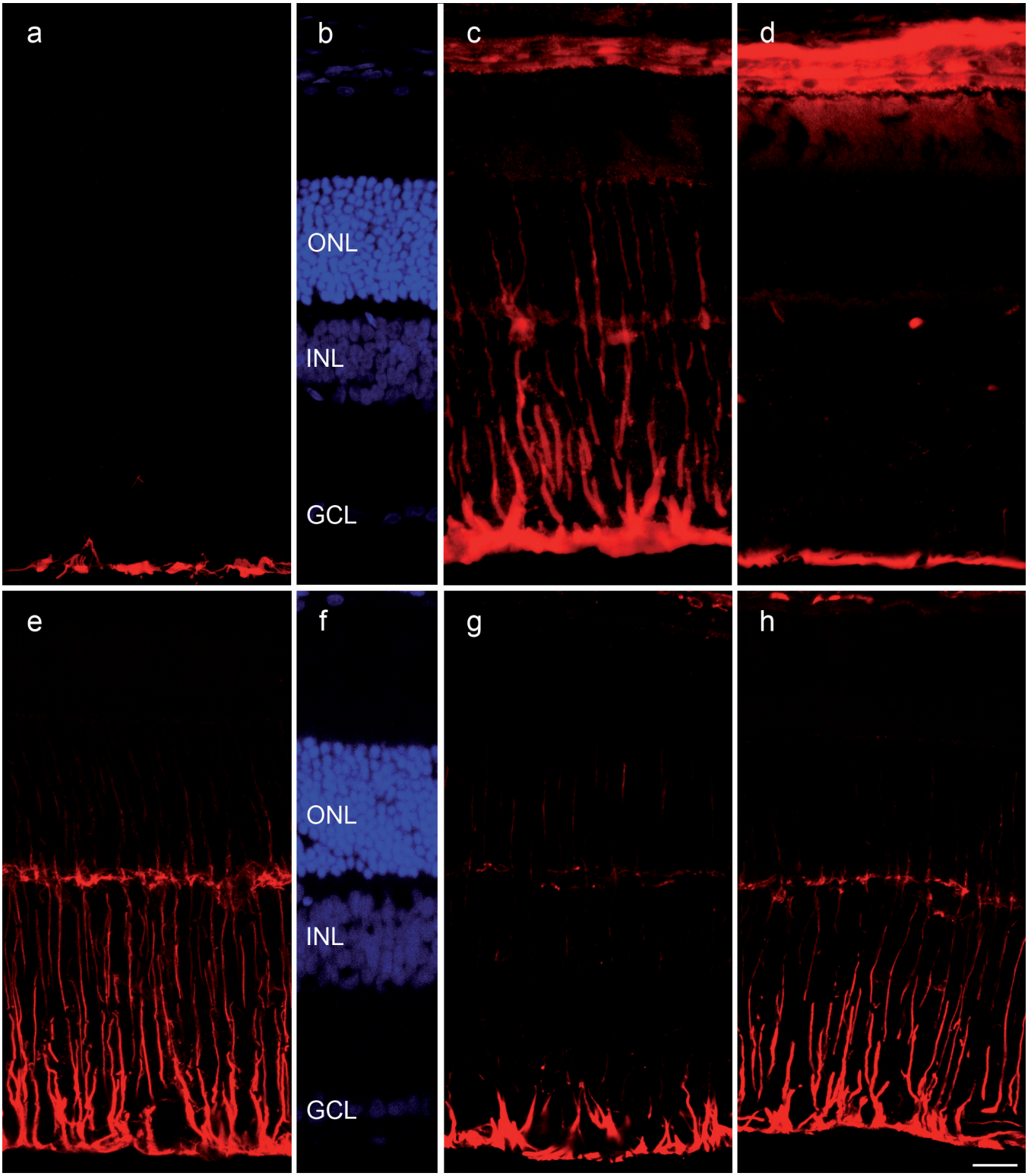

Fig. 1. GFAP and vimentin expression in control and diabetic retinal cryosections. In control rats GFAP staining is prominent only in the ILM **(a)**. In diabetic retinas GFAP upregulation is evident in some regions **(c)**, while almost no glia activation is seen in others **(d)**. Vimentin stains whole Müller glia cells in controls **(e).** The staining intensity is decreased in some **(g)**, but not all regions of the diabetic retina **(h)**. DAPI nuclear staining is provided for overview of the layers **(b, f)**. ONL outer nuclear layer, INL inner nuclear layer, GCL ganglion cell layer. Bar: 20 µm.

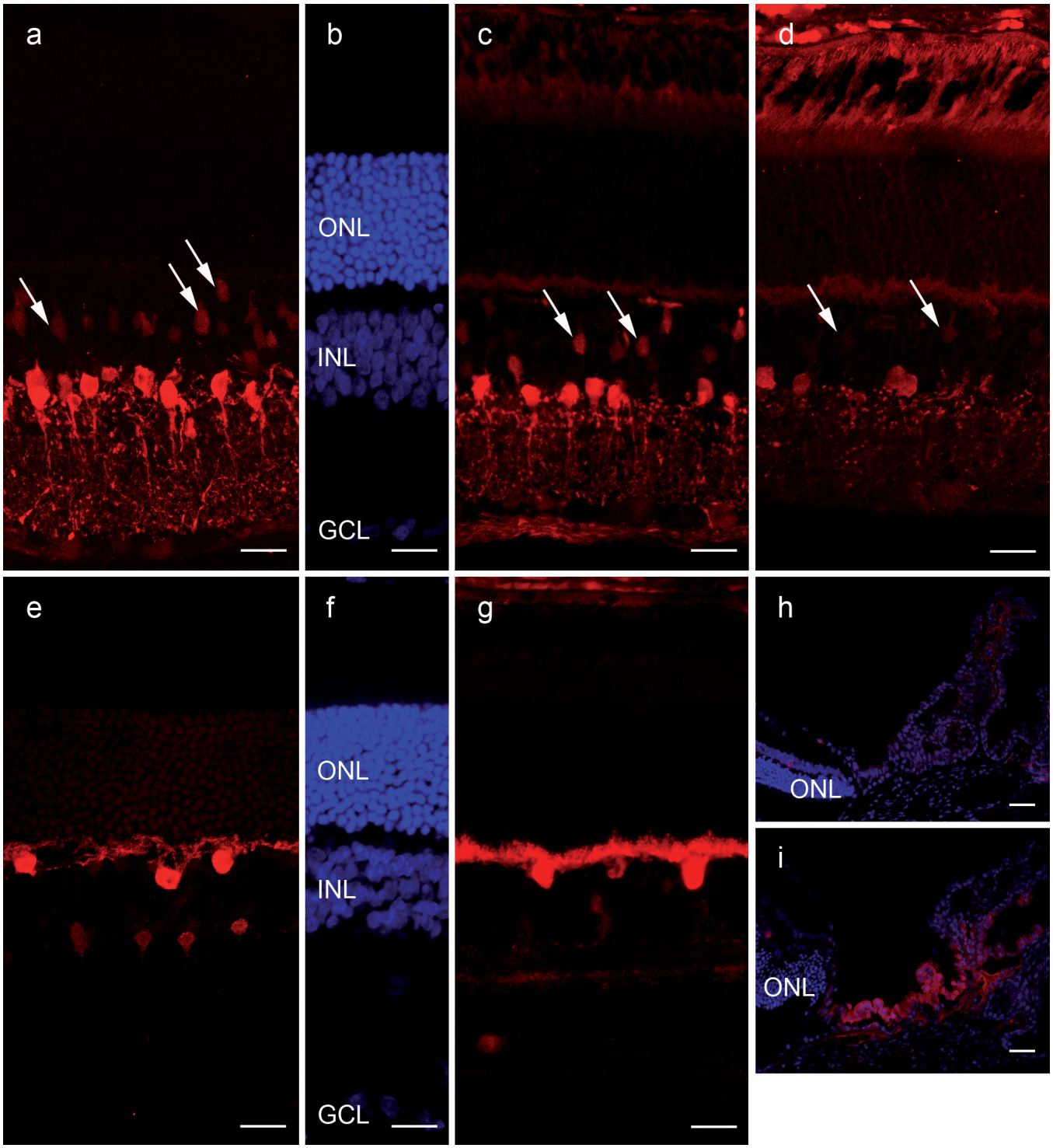

Fig. 2. Labeling pattern of parvalbumin and calbindin in control and diabetic retinas. Parvalbumin stains intensively AII amacrine cells and faintly some bipolar cells (arrows). Compared to controls **(a)**, the staining intensity decreases in certain regions (**d**), while in some other regions no change is evident **(c)**. Figure 2d was slightly overexposed to reveal the residing staining. Calbindin labels horizontal cells, and also a few amacrine and displaced amacrine cells. Its labeling pattern and immunoreactivity is unchanged in diabetes **(g)** compared to controls **(e)** all through the optic retina. Nuclei were visualized with DAPI nuclear staining **(b, f)**. In contrast, while the ciliary part of the retina lacks calbindin labeling in healthy controls **(h)**, intensive labeling is present in diabetes **(i)** in the inner, non-pigmented layer (calbindin staining in red, DAPI nuclear staining in blue). ONL outer nuclear layer, INL inner nuclear layer, GCL ganglion cell layer. Bar: a-g, 20 μm; h, i, 40 μm

all sections examined. In those locations all cell types showed a decrease in immunoreactivity, without a detectable change in the number of AII amacrine cells (4912±1159 and 5197±711 cells/mm^2 in control and diabetic retinas respectively) or labeled cells in the GCL (96±42 vs 144±105 cells/mm^2) (Fig. 3a). Previous data indicated a nearly 20-fold increase in the number of labeled bipolar cells, with almost no cells detectable in control, but plenty well stained cells in diabetic retinas (Park et al., 2008). Although due to the relatively faint staining of the bipolar cells, no cell counting was attempted; we can clearly conclude, that with the staining method used on our specimen, bipolars were detectable even in control retinas, and no major change could be observed either in the staining intensity, or in the number of bipolar cells labeled.

With *calbindin* staining in control animals, strong immunoreactivity was found in horizontal cells, while some lightly stained elements were also visible in the inner part of the INL and GCL (Fig. 2e). The literature indicates that the latter calbindin-positive cells are probably amacrine and displaced amacrine cells (Hamano et al., 1990).

There was no major change detectable in calbindin staining in diabetic rats when central retinal regions were compared (Fig. 2g). The same cell types were labeled and there was no detectable change in the number of calbindin-positive elements in whole mounted retinas

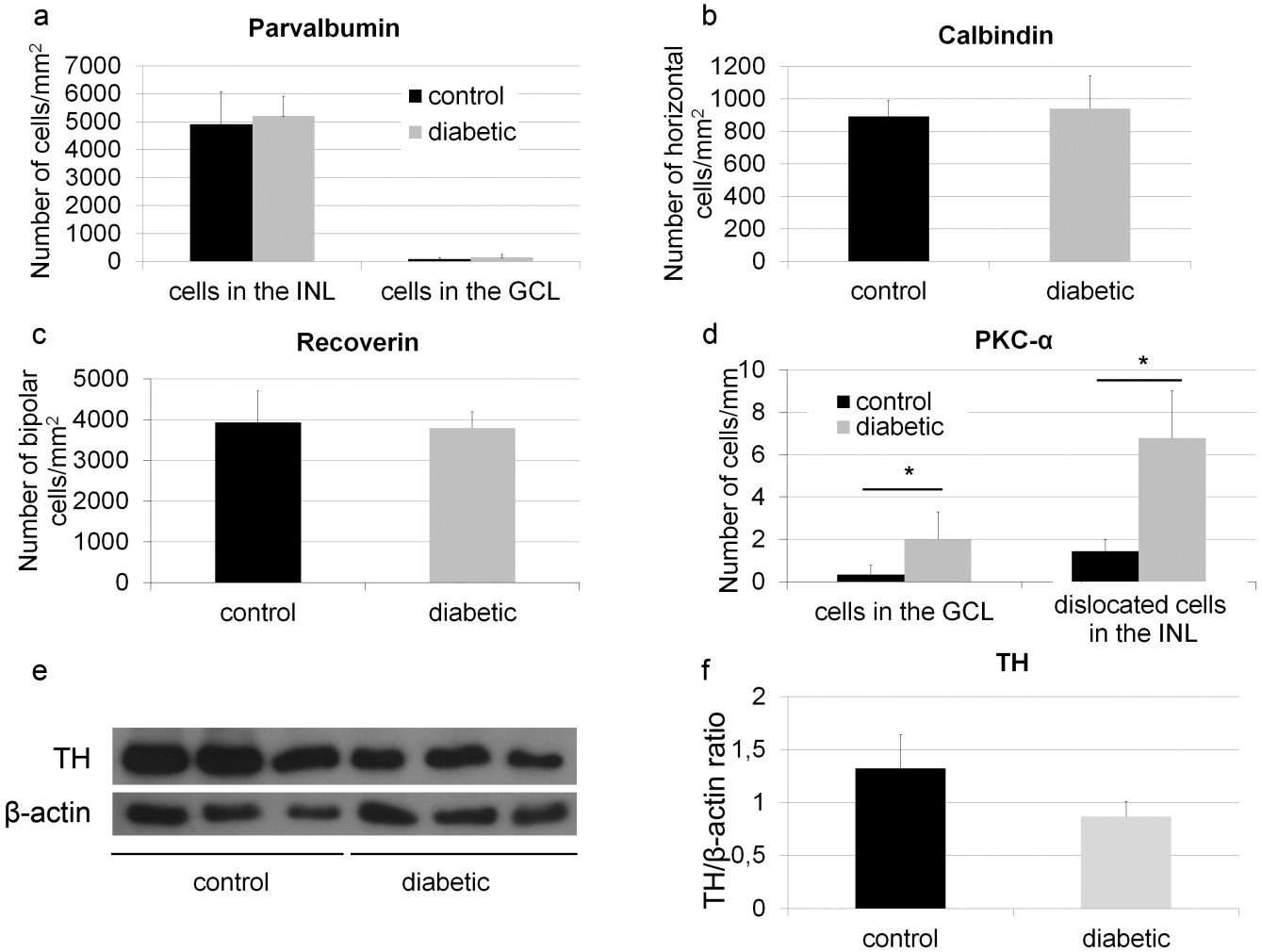

Fig. 3. Quantitative data of whole mounted retinas labeled with parvalbumin, calbindin, recoverin, PKC-α and TH. The number of parvalbumin-positive cells **(a)** in the INL and GCL, calbindin-positive horizontal cells **(b)** and recoverin-positive bipolar cells **(c)** shows no significant reduction or elevation after 12 weeks of diabetes compared to healthy controls. On the contrary, the number of PKC-α-positive cells in the GCL and PKC-α-positive dislocated cells in the INL **(d)** are significantly higher in diabetes than in control. Western blotting **(e)** was used to demonstrate the protein levels of TH and β-actin in healthy and diabetic retinas. TH/β-actin optical density ratios **(f)** confirmed that TH level decreased, however the change was statistically insignificant.* $p<0.05$, INL inner nuclear layer, GCL ganglion cell layer.

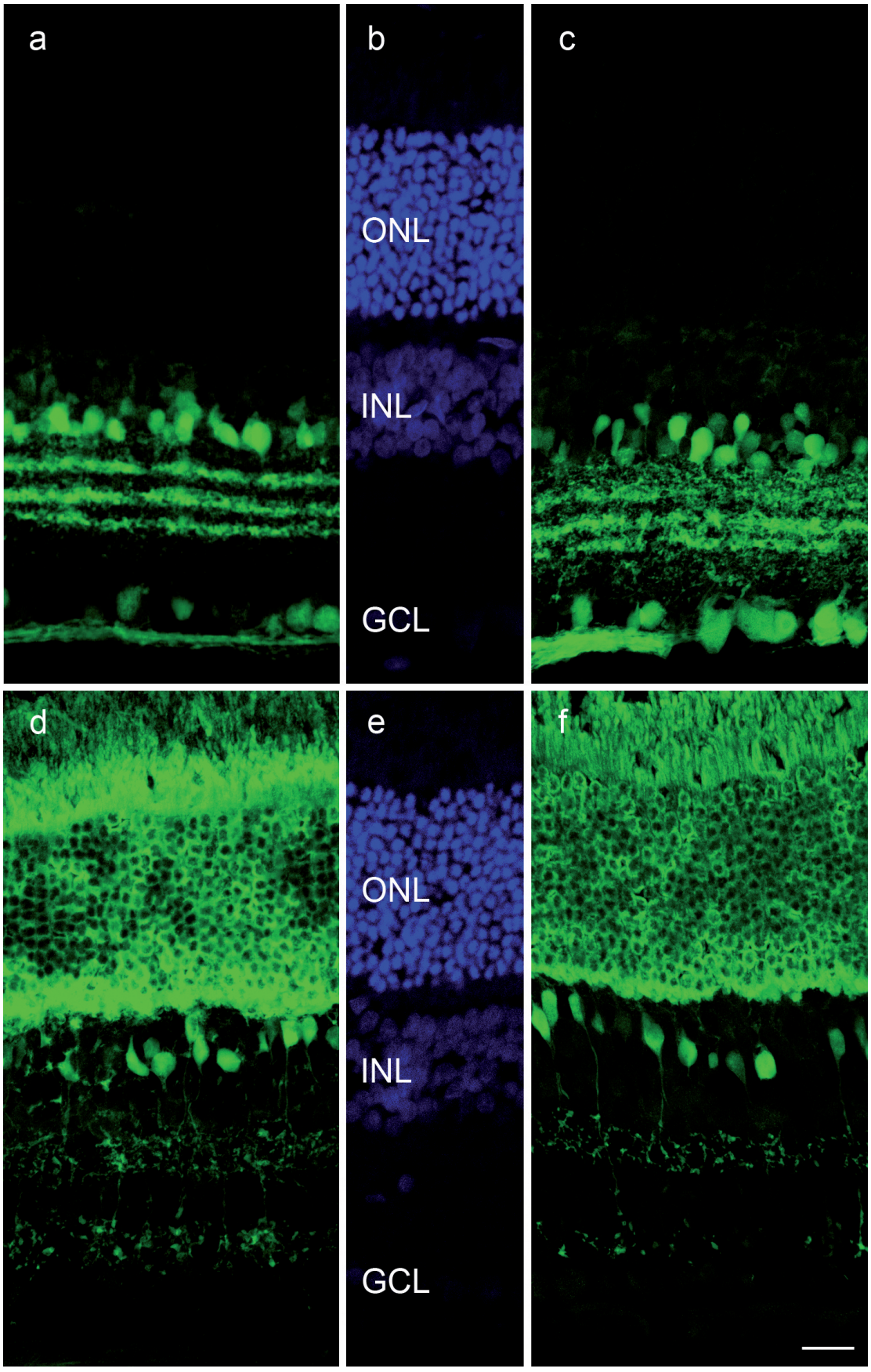

Fig. 4. Calretinin and recoverin expression in control and diabetic rat retinal sections. No alterations could be detected regarding the number of cells and staining intensity, when the labeling of calcium binding proteins calretinin and recoverin in diabetes (calretinin, **c**, recoverin, **f**) was compared to controls (calretinin, **a**, recoverin, **d**). DAPI nuclear staining is provided for overview of the layers **(b, f)**. ONL outer nuclear layer, INL inner nuclear layer, GCL ganglion cell layer. Bar: 20 μm.

(892±97 and 941±200 cells/mm^2 in control and diabetic specimen respectively – Fig. 3b). On the contrary, at the extreme periphery, the inner cell layer of the ciliary part of the retina corresponding to the pars plana of the ciliary body was intensely stained in diabetic rats (Fig. 2i). This feature was present all over the retinal circumference in all diabetic specimens examined, but was never detectable in control retinas (Fig. 2h).

Calretinin is a frequently used marker for amacrine and displaced amacrine cells, with processes terminating in three distinct layers of the IPL (Osborne and Larsen, 1996; Hwang et al., 2005). These features are in concordance with our data in control animals. Comparing calretinin stained sections of control (Fig. 4a) and diabetic (Fig. 4c) rat retinas, no major change was evident.

Recoverin is a well-known marker for ON and OFF cone bipolar cells, also labeling all types of photoreceptors and a few cells in the GCL. Literature data suggest that recoverin-positive cells in the GCL may contain rod or cone opsins and are probably capable of phototransduction (McGinnis et al., 1997). Comparing control and diabetic retinas no major difference in recoverin labeling could be detected in the labeling pattern of photoreceptor cells, cone bipolar cells or cells in the GCL (Fig. 4d,e). Also, there was no change in the number of recoverin-positive cells in the INL on control and diabetic whole mounted retinas counted (3932±773 and 3798±396 cells/mm^2 – Fig. 3c). We observed, however, characteristic changes in the morphology of the axon terminals and synapses of recoverin-positive cone-bipolar cells. Figure 4f demonstrates that the terminal branching of the cells is less elaborate, and the synaptic terminals are unequivocally swollen in diabetic retinas.

Rod bipolar cells in diabetic retinas (PKC-α)

In agreement with the literature, PKC-α labels dominantly rod bipolar cells in control rats along with a few, most probably amacrine or displaced amacrine cells, present only in a very small number (Greferath et al., 1990) (Fig. 5a). In the present study, characteristic changes in the labeling pattern of PKC-α could be observed in diabetic rats (Fig. 5c). Besides rod bipolar cells, at least two other populations of cells (most

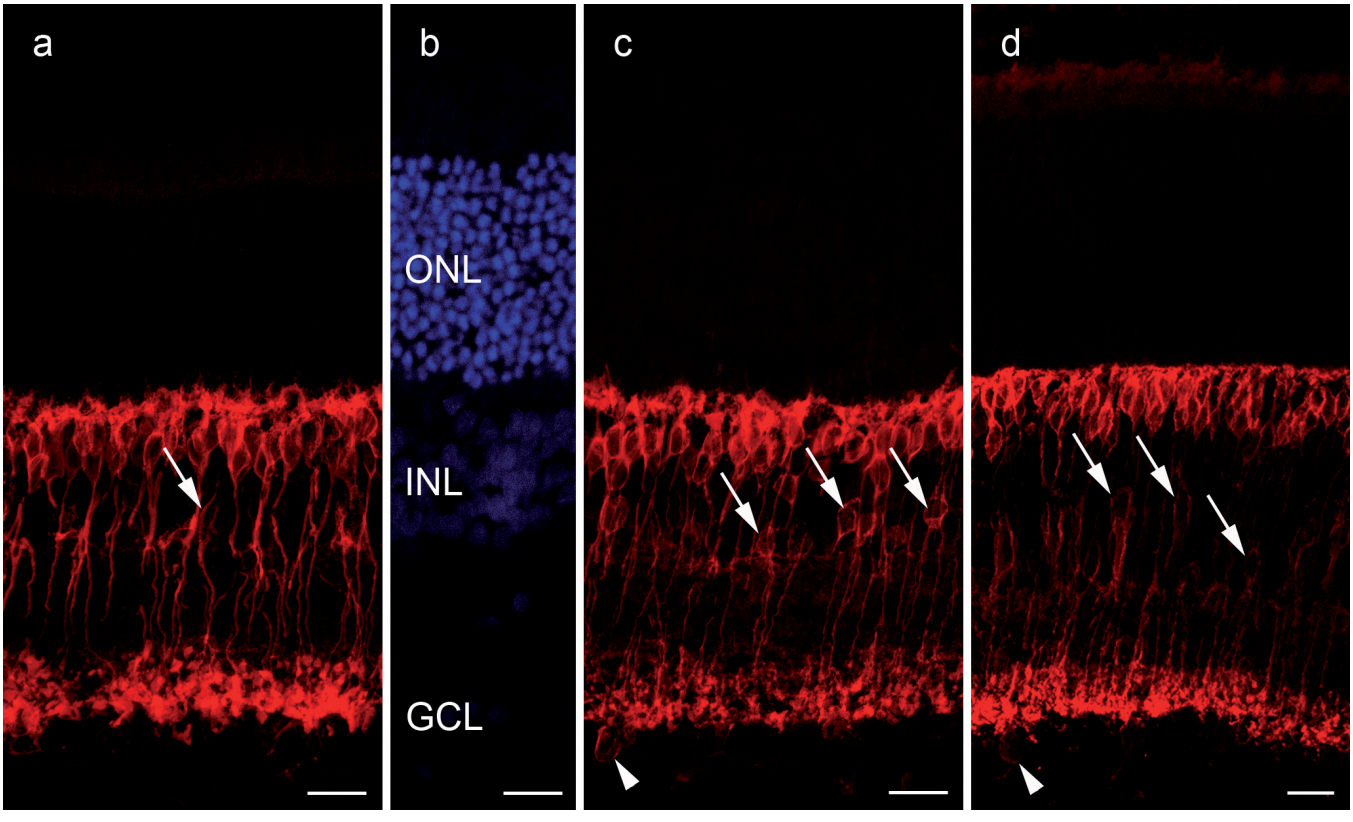

Fig. 5. Representative photos of PKC-α staining on sections of control, diabetic and developing (two-week-old) rats. Arrows indicate a stained population of amacrine cells in the INL, which appears in significantly higher number in diabetes **(c)** compared to controls **(a).** The diabetic retinas show striking similarity to two-week-old specimen **(d).** Arrowheads indicate labeled cells in the ganglion cell layer. Nuclei were visualized with DAPI nuclear staining **(b)**. ONL outer nuclear layer, INL inner nuclear layer, GCL ganglion cell layer. Bar: 20 μm.

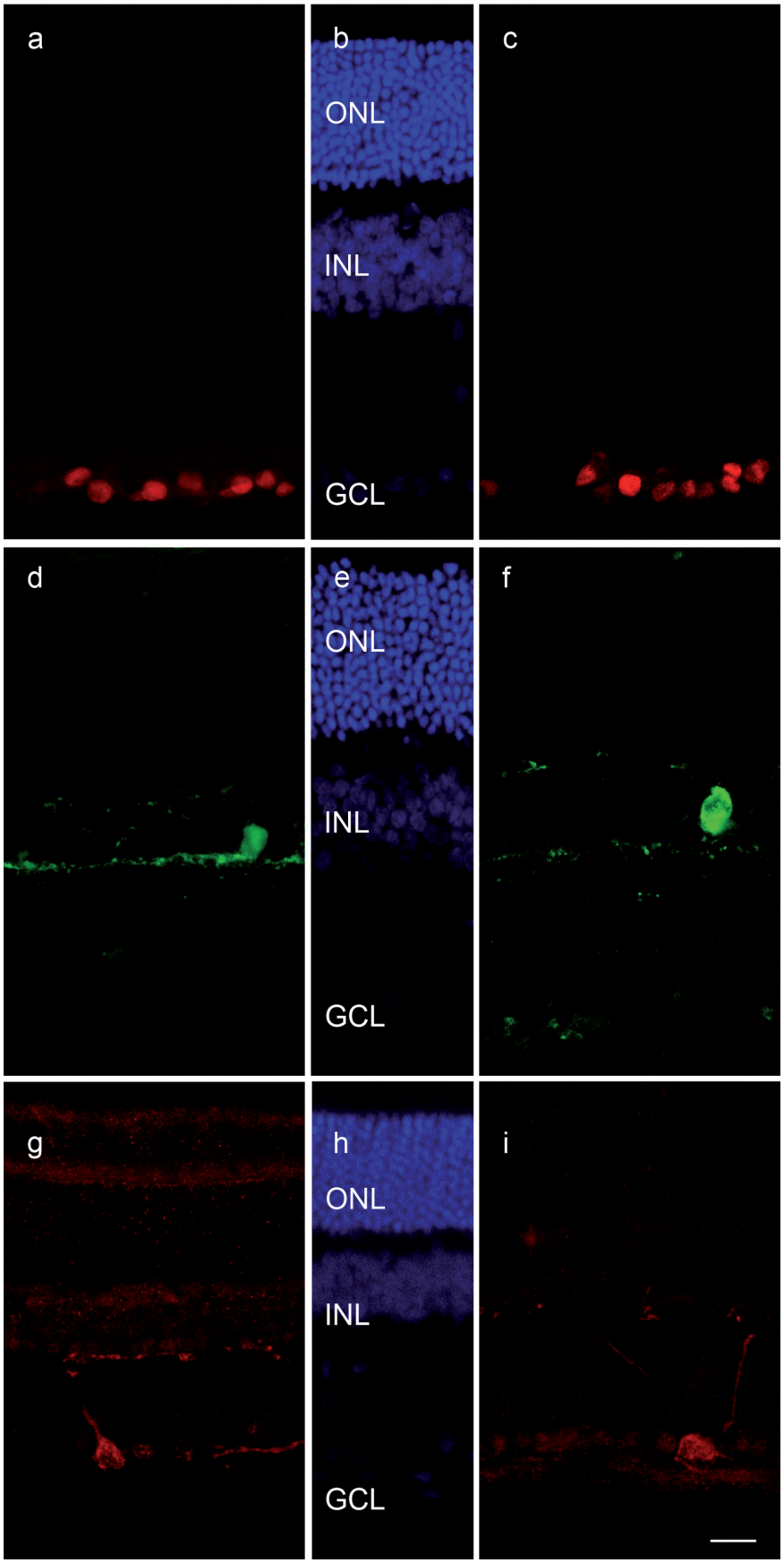

Fig. 6. Representative photomicrographs labeled with anti-Brn-3a, tyrosine hydroxylase (TH) and melanopsin in control and diabetic retinas. Staining with anti-Brn-3a (upper row), TH (middle row) and melanopsin (lower row) is demonstrated. No major alterations could be detected between diabetic **(c, f, i)** and control retinas **(a, d, g)**. Middle column demonstrates DAPI nuclear staining for overview of the layers. ONL outer nuclear layer, INL inner nuclear layer, GCL ganglion cell layer. Bar: 20 µm.

probably amacrine cells) in the INL were also detectable. They were present in significantly higher numbers (6.8±2.2 cells/mm of section length in diabetes vs 1.4±0.5 cells/mm in controls – Fig. 3d). Cells in the GCL (most probably displaced amacrine cells) immunoreactive for PKC-α were also detectable in higher numbers (0.3±0.4 cells/mm in control vs 2.0±1.3 cells/mm in diabetes – Fig. 3d). Interestingly, the appearance of diabetic retinas stained with PKC-α was very similar to what has already been described during rat retinal development (Szabó et al., 2014) (Fig. 5d).

Ganglion cells and amacrine cells (anti-Brn-3a, TH, melanopsin)

TH is a well documented marker for dopaminergic amacrine cells (Nguyen-Legros et al., 1997). Despite a slight decrease in the staining intensity of labeled cells and the less elaborate processes visible (Fig. 6f), there was no major change detectable in the morphology and number of TH-positive cells (70 and 75 in control and diabetic retinal halves respectively). Although the number of whole mounted retinas examined did not allow us to perform a detailed statistical analysis, observations on sections from several different animals (n=4) confirmed that there is no major change in number of TH-positive elements. In agreement with morphological data, a slight (not significant) decrease at the protein level was detectable with Western blot (Fig. 3e,f).

Similarly, based on a series of labeled sections, no evident change was observable for melanopsin (intrinsically photosensitive ganglion cells) (Fig. 6g,i) and anti-Brn-3a (labeling the majority of ganglion cells) (Fig. 6a,c) labeling.

Discussion

A series of studies from the last decades have shown that in diabetes neurodegenerative components are present prior to clinically significant vasculopathy, reporting Müller glial reactivity (Rungger-Brändle et al., 2000; Feit-Leichman et al., 2005; van Dijk et al., 2009) and labeling pattern alterations of some other inner retinal elements, including dopaminergic and AII amacrine cells (Ng et al., 2004; Seki et al., 2004; Szabadfi et al., 2012). In the literature there is general agreement that loss of ganglion cells and inner retinal layer cell types occur in diabetic rats. However, the onset of decreased thickness of inner layers and the significant loss of ganglion cells depend on experimental circumstances: the time of detection has a range between 4 weeks and 9 months after diabetes induction (Kern and Barber, 2008).

In a previous report (Enzsöly et al., 2014) 12 weeks after diabetes induction, using the same specimens, we demonstrated changes in opsin expression, outer segment morphology and retinal pigment epithelial degeneration. We also showed that the thickness of the whole retina and the ONL alone was unchanged, there was no increase in the number of TUNEL-positive elements in diabetes compared to controls and no loss of photoreceptor cells was detectable. In the present study we demonstrated that none of the inner layer cell types analyzed showed any significant decrease in their number. Added together, all these data clearly indicate that the early diabetic alterations presented here precede significant apoptotic loss of cells.

Based on our present observations, three major points should be highlighted. 1) We demonstrated, for the first time, that some, but not all of the antibodies used (GFAP, vimentin, parvalbumin) outlined randomly distributed regions with detectable retinal lesions, while other regions were devoid of any significant change. 2) Labeling with TH clearly demonstrated that some of the changes described by others in earlier stages of the disease (2-4 weeks after the induction of diabetes (Seki et al., 2004; Szabadfi et al., 2012)), like decrease in the number of TH immunopositive dopaminergic amacrine cells detectable, could be transitional as these changes were not present in the retinas examined in this study. 3) PKC-α and calbindin labeling revealed patterns reminiscent of those found in developing retinas. The results will be discussed following these three major points.

1) Among the many changes that have been described in Müller cells under diabetic conditions, gliosis is one of the earliests. There is evidence in the literature for increased GFAP expression even as early as 1 month after the induction of diabetes (Lieth et al., 1998), although the onset and range of labeling may vary under different experimental conditions. Labeling for GFAP in experimentally induced diabetes is reported to range from a signal restricted to the inner limiting membrane (Feit-Leichman et al., 2005) to labeling the whole glial cell (Lieth et al., 1998). The upregulation of GFAP is proposed to occur transiently in a mouse model of diabetes (Feit-Leichman et al., 2005). It was also reported that the development of gliosis is uneven, initially beginning at the periphery and later central regions become involved (Ly et al., 2011). In a detailed report by Rungger-Brändle et al., (2000), GFAP expression was upregulated 12 weeks after diabetes induction, coinciding with an increase in the number of Müller cells, and a decrease in the number of astrocytes detected.

Although the actual number of glia cell types was not estimated in our report, in agreement with the data of others, our results demonstrated an increase in GFAP labeling. On the other hand we can not confirm the periphero-central progression of gliosis. Retinal areas showing an increased GFAP labeling were arranged in a patchy manner, distributed irregularly throughout the retina, with no specific localization to the central or peripheral regions. Also, the lesions were not restricted either to the inferior or to the superior retinal halves. The reason for this discrepancy is unknown, but it is

important to note that even in adult healthy rat retina, peripheral GFAP labeling can often be detected.

Analyzing at least four retinas per group labeled with each antibody, we could not reveal any consequent localization of the diabetic injuries. This indicates that in order to fully analyze the staining pattern of a given antibody, a series of sections prepared from different regions of the retina are required. Sampling only the central retina may result in inconsistent data. Despite these local variations within a given retina, with this detailed analysis, we found a surprisingly low variation between individual animals.

Not only GFAP, but also vimentin and parvalbumin labeling demonstrated damaged retinal regions that were distributed in a similar, seemingly random manner throughout the retina. In vimentin immunoreactivity, we found areas of slightly decreased staining intensities. We are the first to report a decrease in vimentin expression in diabetes, the reason for this finding is currently unknown and we can only speculate about it. A recent report by Wang et al. (2011) demonstrated that under in vitro conditions, Müller cells downregulate vimentin expression, while GFAP expression remains normal, in the case of microglia activation (Wang et al., 2011). There are plenty of studies reporting that microglia activation is present in diabetes (Rungger-Brändle et al., 2000; Ibrahim et al., 2011), even before ganglion cell death (Gaucher et al., 2007) giving a possible explanation to this unexpected result.

In the case of parvalbumin we also detected patches of less intense labeling without any significant change in the number of labeled cells. In the literature there is evidence for a marked elevation in the number of parvalbumin-positive cells after 16 weeks of diabetes (Ng et al., 2004), while in another report no change in the number of AII amacrine cells was observed after 12 weeks (Park et al., 2008). None of these authors reported any difference confined to specific retinal regions. Park et al. (2008) reported a more than twentyfold increase in the number of parvalbumin labeled bipolar cells after 12 weeks of diabetes. In our cryosections, bipolar cells were regularly detected even in control specimens, and we can definitely conclude that there was no obvious increase in their number under diabetic conditions.

We must point out that the uneven distribution of diabetic injuries in this experimental setup was restricted to certain cell-type specific markers. In contrast to GFAP, vimentin and parvalbumin, no noteworthy changes could be detected with recoverin and calretinin staining, while in the case of PKC-α the changes were evident throughout the whole retina, without any local variations. The changes in calbindin staining were restricted to the ciliary part of the retina. All these data demonstrate clearly that this finding of patchy degeneration is not an artifact, but rather a regional response of certain retinal cell types to diabetic conditions, probably before the whole retina is affected in later stages of the disease. The patchy localization of the altered retinal areas cannot be explained at present and further studies are needed to find a possible cause for the development of this uneven reactivity. It cannot be excluded that the patchy pattern is related to some fine structural alterations of blood vessels, like microangiopathy or changes in blood supply.

Interestingly, amongst the many calcium binding proteins (including parvalbumin, calbindin, calretinin and recoverin), frequently used to selectively label certain types of cells in the inner layers of the retina, only parvalbumin showed any change in staining intensity. These proteins are supposed to function as calcium buffers having important roles in maintaining the calcium homeostasis in the neural retina. During certain metabolic conditions e.g. diabetes, excessive glutamate level causes an increase in the intracellular level of calcium, which induces potentially neurotoxic processes. Therefore, the role of calcium binding proteins in retinal injuries, including diabetic retinopathy, may be critical (Agardh et al., 2001; Ng et al., 2004, Park et al., 2008). Immunohistochemical data on changes of parvalbumin, calbindin, calretinin and recoverin are available in animal models of ischemic, oxygen-induced retinopathy and photoreceptor degeneration (Cuenca et al., 2004; Yamamoto et al., 2006; Hernandez et al., 2009; Kim et al., 2010; Dorfman et al., 2011; Lee et al., 2011). In diabetes however, only the staining of parvalbumin (staining mostly AII amacrine cells) was shown to change (Park et al., 2008). In our study, the change in the staining of parvalbumin was manifested by regions of decreased immunoreactivity. This may indicate a decrease in calcium binding capacity, thus AII amacrine cells could be more vulnerable under diabetic conditions. AII amacrine cells have diverse proven and supposed functions: besides being the major modulator cells in the route of rod signals towards bipolar cells, they also function under scotopic conditions, they help to increase signal to noise ratio and so on (for a recent review see: (Demb and Singer, 2012)). Reduced oscillatory potentials are among the abnormalities of early diabetic electroretinogram findings (Aizu et al., 2002; Luu et al., 2010), which are considered to suggest dysfunction of amacrine cells, although not specific to type AII. Furthermore, in a recent report by Pardue et al. implicit times and amplitudes of scotopic oscillatory potentials were reported to change earlier than photopic ERG signals (Pardue et al., 2014), suggesting alteration of the rod signal route in early diabetes, with the probable involvement of AII amacrine cells. The precise description of the pathology of this celltype requires further studies and is beyond the scope of the present paper.

2) There are several data in the literature that retinal dopaminergic homeostasis is affected as an early sign of diabetic injury. The number of dopaminergic amacrine cells detectable with immunohistochemistry and also the protein level of TH were reported to be reduced 3 and 4 weeks after the induction of diabetes (Seki et al., 2004;

Szabadfi et al., 2012). Furthermore, supporting morphological data, some alterations on the electroretinogram were thought to reflect dysfunctions of the dopaminergic system in early diabetes (Shirao and Kawasaki, 1998). Therefore, it was important to investigate TH immunoreactivity in our experimental setup as well.

Here, in line with other reports, the intensity of TH immunostaining of dopaminergic amacrine cells was found to be slightly weaker in diabetic retinas, although quantitatively no significant reduction could be revealed either in the number of cells or in the protein levels. The discrepancy between our study and others may lie in the different duration of induced diabetes, which was 12 weeks in our present study, while only 3 and 4 weeks in other reports (Seki et al., 2004; Szabadfi et al., 2012). As the induction method was practically identical, we must propose that shortly after the diabetes induction cells were damaged (demonstrated by their decreased staining intensity, which may be beyond detectability), then later somehow recovered, regained original TH content and possibly restored normal functions as well. Despite the decrease in immunoreactivity, most dopaminergic cells can seemingly survive diabetic conditions for the relatively long period of 12 weeks according to our results, and after initial damage, possibly recover with a near normal protein content and morphology. The original damage may be due to the metabolic shock or the direct neurotoxicity of STZ. Alternatively, we can also explain our results by assuming cell proliferation that restores normal cell numbers, but at this stage we lack any direct evidence supporting this idea.

3) Another interesting observation of this study was that certain retinal markers showed labeling patterns which were otherwise characteristic for the developing retina. The staining of PKC-α in diabetes shows a close resemblance to that of the retina under development (Szabó et al., 2014). Besides being a specific marker for rod bipolar cells, PKC-α also labels a small population of amacrine cells in the INL, and a few supposedly displaced amacrine cells in the GCL. These cells were shown to be GABAergic in rats, but to the best of our knowledge, precise identification of these amacrine cells is still missing. Although the role of PKC has been widely studied and the distribution of different isoforms was described in detail in rats, the function of the PKC-α positive amacrine cells in the INL is still undiscovered.

In our diabetic specimens no change was evident concerning rod bipolar cells, while the labeled population of amacrine cells was represented in a much higher number, with an approximately fourfold increase detectable. The ratio of bipolars to amacrine cells with PKC-α labeling was similar to what was seen during early postnatal development. The morphology of positive amacrine cells detected in diabetes, within the limitations of the detection technique, was not different compared to controls. This could be explained by assuming remodeling or some compensation for the compromised functions of the retina: some amacrine cells may change the expression pattern of PKC-α to adjust functions to the needs of the changing/damaged retina. Alternatively, cell proliferation could also give an explanation for this phenomenon.

Also, in a previous report (Enzsöly et al., 2014) on diabetic rats, we detected an increase in the number of dual cones, coexpressing both S- and M/L-opsins, especially in the peripheral retina. Such elements regularly appear during the first two or three weeks of postnatal development in some mammals, including rats (Szél et al., 1994). They were also detected during human retinal maturation (Xiao and Hendrickson, 2000). In the rat retina, at birth all cones express blue-opsin only, but later the majority of the cone population switches to producing M- (or in case of humans also L-) opsins and transdifferentiate to the definitive M- or L-cone type. In the state of transition cones contain both opsins for a limited time interval. Dual cones may also be present in adult retinas, albeit usually in extremely small numbers (Lukáts et al., 2005). This previous work demonstrated an almost tenfold increase in the number of dual cones in diabetic rats compared to controls (Enzsöly et al., 2014). Interestingly, despite the outstanding outer segment degeneration detected in this specimen, the total number of cones did not change significantly, therefore we raised the possibility that new cones are created, differentiated and integrated into the photoreceptor mosaic under diabetic conditions and the dual elements represent the transdifferentiation stage of cone development.

In line with these observations, the unexpected recovery of TH staining discussed above, the altered labeling pattern of PKC-α staining, with increased number of amacrine cells, similarly to the developing retina, and the increase in the number of Müller cells detected by Rungger-Brändle et al. (2000) can theoretically be explained alternatively, by assuming cell proliferation. Furthermore, another specific change resembling the developing retina was demonstrated in the ciliary part of retina in diabetes with calbindin labeling: intensive labeling appeared in the inner, non-pigmented layer of cells. In certain submammalian species, the ciliary retina contains stem cells that are continuously dividing and are responsible for the growing and regeneration of the retina (Reh and Fischer, 2001; Cid et al., 2002). There is some evidence for the presence of stem cells in the ciliary part of the retina also in mammals (Tropepe et al., 2000). Changes in diabetes affecting calbindin expression of the ciliary retina may reflect an increase in stem cell activity, but further future studies are needed to confirm this possibility.

All these data strengthen the idea that regenerative capacity may be present in diabetes. We must admit however, that all this evidence is indirect, and there is an urge for further studies to confirm or rule out this possibility.

In conclusion, we have shown that signs of early diabetic neurodegeneration are clearly and reproducibly

detectable also in the inner retina, prior to significant apoptotic loss of cells, or expectable vasculopathy. The changes first appear in a patchy manner for several markers before possibly affecting the whole retina. Our results also raise the possibility that some of the alterations described in earlier stages of the disease are transitional, and a significant regenerative capacity may be present, possibly with even cell proliferation involved.

In the light of our results showing reproducible alterations in some of the neural and glial elements, application of an additional neuroprotective therapy should be considered and tested on diabetic specimen. As demonstrated by Sasase et al. (2009) for example, some of the functional alterations of the diabetic retina can indeed be prevented.

Further studies are required to get further insights into the pathomechanisms and the functional consequences of these observations.

Acknowledgements. This work was supported by the Hungarian Scientific Research Fund (OTKA #73000) and TÁMOP- 4.2.1.B-09/1KMRB2010-0001.

The authors thank Professor Pál Röhlich for the critical reading of the manuscript.

References

Agardh E., Bruun A. and Agardh C.D. (2001). Retinal glial cell immunoreactivity and neuronal cell changes in rats with stz-induced diabetes. Curr. Eye Res. 23, 276-284.

Aizu Y., Oyanagi K., Hu J. and Nakagawa H. (2002). Degeneration of retinal neuronal processes and pigment epithelium in the early stage of the streptozotocin-diabetic rats. Neuropathology 22, 161-170.

Anderson H.R., Stitt A.W., Gardiner T.A. and Archer D.B. (1995). Diabetic retinopathy: Morphometric analysis of basement membrane thickening of capillaries in different retinal layers within arterial and venous environments. Br. J. Ophthalmol. 79, 1120-1123.

Antonetti D.A., Klein R. and Gardner T.W. (2012). Diabetic retinopathy. N. Engl. J. Med. 366, 1227-1239.

Antonetti D.A., Barber A.J., Bronson S.K., Freeman W.M., Gardner T.W., Jefferson L.S., Kester M., Kimball S.R., Krady J.K., LaNoue K.F., Norbury C.C., Quinn P.G., Sandirasegarane L., Simpson I.A. and Group J.D.R.C. (2006). Diabetic retinopathy: Seeing beyond glucose-induced microvascular disease. Diabetes 55, 2401-2411.

Aung M.H., Kim M.K., Olson D.E., Thule P.M. and Pardue M.T. (2013). Early visual deficits in streptozotocin-induced diabetic long evans rats. Invest. Ophthalmol. Vis. Sci. 54, 1370-1377.

Barber A.J., Lieth E., Khin S.A., Antonetti D.A., Buchanan A.G. and Gardner T.W. (1998). Neural apoptosis in the retina during experimental and human diabetes. Early onset and effect of insulin. J. Clin. Invest. 102, 783-791.

Bearse M.A., Adams A.J., Han Y., Schneck M.E., Ng J., Bronson-Castain K. and Barez S. (2006). A multifocal electroretinogram model predicting the development of diabetic retinopathy. Prog. Retin. Eye. Res. 25, 425-448.

Bradford M.M. (1976). A rapid and sensitive method for the quantitation of microgram quantities of protein utilizing the principle of protein-dye binding. Anal. Biochem. 72, 248-254.

Chun M.H., Kim I.B., Ju W.K., Kim K.Y., Lee M.Y., Joo C.K. and Chung J.W. (1999). Horizontal cells of the rat retina are resistant to degenerative processes induced by ischemia-reperfusion. Neurosci. Lett. 260, 125-128.

Cid E., Velasco A., Ciudad J., Orfao A., Aijón J. and Lara J.M. (2002). Quantitative evaluation of the distribution of proliferating cells in the adult retina in three cyprinid species. Cell Tissue Res. 308, 47-59.

Cuenca N., Pinilla I., Sauvé Y., Lu B., Wang S. and Lund R.D. (2004). Regressive and reactive changes in the connectivity patterns of rod and cone pathways of p23h transgenic rat retina. Neuroscience 127, 301-317.

Curtis T.M., Gardiner T.A. and Stitt A.W. (2009). Microvascular lesions of diabetic retinopathy: Clues towards understanding pathogenesis? Eye (Lond) 23, 1496-1508.

Demb J.B. and Singer J.H. (2012). Intrinsic properties and functional circuitry of the aII amacrine cell. Vis. Neurosci. 29, 51-60.

Dorfman A.L., Cuenca N., Pinilla I., Chemtob S. and Lachapelle P. (2011). Immunohistochemical evidence of synaptic retraction, cytoarchitectural remodeling, and cell death in the inner retina of the rat model of oygen-induced retinopathy (OIR). Invest. Ophthalmol. Vis. Sci. 52, 1693-1708.

Enzsöly A., Szabó A., Kántor O., Dávid C., Szalay P., Szabó K., Szél A., Németh J. and Lukáts A. (2014). Pathologic alterations of the outer retina in streptozotocin-induced diabetes. Invest. Ophthalmol. Vis. Sci. 55, 3686-3699.

Feit-Leichman R.A., Kinouchi R., Takeda M., Fan Z., Mohr S., Kern T.S. and Chen D.F. (2005). Vascular damage in a mouse model of diabetic retinopathy: Relation to neuronal and glial changes. Invest. Ophthalmol. Vis. Sci. 46, 4281-4287.

Gaucher D., Chiappore J.A., Pâques M., Simonutti M., Boitard C., Sahel J.A., Massin P. and Picaud S. (2007). Microglial changes occur without neural cell death in diabetic retinopathy. Vision Res. 47, 612-623.

Greferath U., Grünert U. and Wässle H. (1990). Rod bipolar cells in the mammalian retina show protein kinase c-like immunoreactivity. J. Comp. Neurol. 301, 433-442.

Hamano K., Kiyama H., Emson P.C., Manabe R., Nakauchi M. and Tohyama M. (1990). Localization of two calcium binding proteins, calbindin (28 kd) and parvalbumin (12 kd), in the vertebrate retina. J. Comp. Neurol. 302, 417-424.

Hattar S., Liao H.W., Takao M., Berson D.M. and Yau K.W. (2002). Melanopsin-containing retinal ganglion cells: Architecture, projections, and intrinsic photosensitivity. Science 295, 1065-1070.

Hernandez M., Rodriguez F.D., Sharma S.C. and Vecino E. (2009). Immunohistochemical changes in rat retinas at various time periods of elevated intraocular pressure. Mol. Vis. 15, 2696-2709.

Hwang I.K., Yoo K.Y., Kim D.S., Jung J.Y., Shin M.C., Seo K., Kim K.S., Kang T.C. and Won M.H. (2005). Comparative study on calretinin immunoreactivity in gerbil and rat retina. Anat. Histol. Embryol. 34, 129-131.

Ibrahim A.S., El-Remessy A.B., Matragoon S., Zhang W., Patel Y., Khan S., Al-Gayyar M.M., El-Shishtawy M.M. and Liou G.I. (2011). Retinal microglial activation and inflammation induced by amadori-glycated albumin in a rat model of diabetes. Diabetes 60, 1122-1133.

Kern T.S. and Barber A.J. (2008). Retinal ganglion cells in diabetes. J. Physiol. 586, 4401-4408.

Kim S.A., Jeon J.H., Son M.J., Cha J., Chun M.H. and Kim I.B. (2010). Changes in transcript and protein levels of calbindin d28k, calretinin

and parvalbumin, and numbers of neuronal populations expressing these proteins in an ischemia model of rat retina. Anat. Cell Biol. 43, 218-229.

Lai A.K. and Lo A.C. (2013). Animal models of diabetic retinopathy: Summary and comparison. J. Diabetes Res. 2013, 106594.

Lee J.H., Shin J.M., Shin Y.J., Chun M.H. and Oh S.J. (2011). Immunochemical changes of calbindin, calretinin and smi32 in ischemic retinas induced by increase of intraocular pressure and by middle cerebral artery occlusion. Anat. Cell Biol. 44, 25-34.

Lieth E., Barber A.J., Xu B., Dice C., Ratz M.J., Tanase D. and Strother J.M. (1998). Glial reactivity and impaired glutamate metabolism in short-term experimental diabetic retinopathy. Penn state retina research group. Diabetes 47, 815-820.

Lukáts A., Szabó A., Röhlich P., Vígh B. and Szél A. (2005). Photopigment coexpression in mammals: Comparative and developmental aspects. Histol. Histopathol. 20, 551-574.

Luu C.D., Szental J.A., Lee S.Y., Lavanya R. and Wong T.Y. (2010). Correlation between retinal oscillatory potentials and retinal vascular caliber in type 2 diabetes. Invest. Ophthalmol. Vis. Sci. 51, 482-486.

Ly A., Yee P., Vessey K.A., Phipps J.A., Jobling A.I. and Fletcher E.L. (2011). Early inner retinal astrocyte dysfunction during diabetes and development of hypoxia, retinal stress, and neuronal functional loss. Invest. Ophthalmol. Vis. Sci. 52, 9316-9326.

Martin P.M., Roon P., Van Ells T.K., Ganapathy V. and Smith S.B. (2004). Death of retinal neurons in streptozotocin-induced diabetic mice. Invest. Ophthalmol. Vis. Sci. 45, 3330-3336.

McGinnis J.F., Stepanik P.L., Jariangprasert S. and Lerious V. (1997). Functional significance of recoverin localization in multiple retina cell types. J. Neurosci. Res. 50, 487-495.

Nadal-Nicolás F.M., Jiménez-López M., Sobrado-Calvo P., Nieto-López L., Cánovas-Martínez I., Salinas-Navarro M., Vidal-Sanz M. and Agudo M. (2009). Brn3a as a marker of retinal ganglion cells: Qualitative and quantitative time course studies in naive and optic nerve-injured retinas. Invest. Ophthalmol. Vis. Sci. 50, 3860-3868.

Ng Y.K., Zeng X.X. and Ling E.A. (2004). Expression of glutamate receptors and calcium-binding proteins in the retina of streptozotocin-induced diabetic rats. Brain Res. 1018, 66-72.

Nguyen-Legros J., Versaux-Botteri C. and Savy C. (1997). Dopaminergic and GABAergic retinal cell populations in mammals. Microsc. Res. Tech. 36, 26-42.

Osborne N.N. and Larsen A.K. (1996). Antigens associated with specific retinal cells are affected by ischaemia caused by raised intraocular pressure: Effect of glutamate antagonists. Neurochem. Int. 29, 263-270.

Pardue M.T., Barnes C.S., Kim M.K., Aung M.H., Amarnath R., Olson D.E. and Thulé P.M. (2014). Rodent hyperglycemia-induced inner retinal deficits are mirrored in human diabetes. Transl. Vis. Sci. Technol. 3, 6.

Park H.S., Park S.J., Park S.H., Chun M.H. and Oh S.J. (2008). Shifting of parvalbumin expression in the rat retina in experimentally induced diabetes. Acta Neuropathol. 115, 241-248.

Reh T.A. and Fischer A.J. (2001). Stem cells in the vertebrate retina. Brain Behav. Evol. 58, 296-305.

Rungger-Brändle E. and Dosso A.A. (2003). Streptozotocin-induced diabetes--a rat model to study involvement of retinal cell types in the onset of diabetic retinopathy. Adv. Exp. Med. Biol. 533, 197-203.

Rungger-Brändle E., Dosso A.A. and Leuenberger P.M. (2000). Glial reactivity, an early feature of diabetic retinopathy. Invest. Ophthalmol. Vis. Sci. 41, 1971-1980.

Sasase T., Morinaga H., Abe T., Miyajima K., Ohta T., Shinohara M., Matsushita M. and Kakehashi A. (2009). Protein kinase c beta inhibitor prevents diabetic peripheral neuropathy, but not histopathological abnormalities of retina in spontaneously diabetic torii rat. Diabetes Obes. Metab. 11, 1084-1087.

Schnitzer J., Franke W.W. and Schachner M. (1981). Immunocytochemical demonstration of vimentin in astrocytes and ependymal cells of developing and adult mouse nervous system. J. Cell Biol. 90, 435-447.

Seki M., Tanaka T., Nawa H., Usui T., Fukuchi T., Ikeda K., Abe H. and Takei N. (2004). Involvement of brain-derived neurotrophic factor in early retinal neuropathy of streptozotocin-induced diabetes in rats: Therapeutic potential of brain-derived neurotrophic factor for dopaminergic amacrine cells. Diabetes 53, 2412-2419.

Shirao Y. and Kawasaki K. (1998). Electrical responses from diabetic retina. Prog. Retin. Eye Res. 17, 59-76.

Szabadfi K., Atlasz T., Kiss P., Reglodi D., Szabo A., Kovacs K., Szalontai B., Setalo G., Banki E., Csanaky K., Tamas A. and Gabriel R. (2012). Protective effects of the neuropeptide pacap in diabetic retinopathy. Cell Tissue Res. 348, 37-46.

Szabó K., Szabó A., Enzsöly A., Szél A. and Lukáts A. (2014). Immunocytochemical analysis of misplaced rhodopsin-positive cells in the developing rodent retina. Cell Tissue Res. 356, 49-63.

Szél A., van Veen T. and Röhlich P. (1994). Retinal cone differentiation. Nature 370, 336.

Tropepe V., Coles B.L., Chiasson B.J., Horsford D.J., Elia A.J., McInnes R.R. and van der Kooy D. (2000). Retinal stem cells in the adult mammalian eye. Science 287, 2032-2036.

van Dijk H.W., Kok P.H., Garvin M., Sonka M., Devries J.H., Michels R.P., van Velthoven M.E., Schlingemann R.O., Verbraak F.D. and Abràmoff M.D. (2009). Selective loss of inner retinal layer thickness in type 1 diabetic patients with minimal diabetic retinopathy. Invest. Ophthalmol. Vis. Sci. 50, 3404-3409.

van Dijk H.W., Verbraak F.D., Kok P.H., Garvin M.K., Sonka M., Lee K., Devries J.H., Michels R.P., van Velthoven M.E., Schlingemann R.O. and Abràmoff M.D. (2010). Decreased retinal ganglion cell layer thickness in patients with type 1 diabetes. Invest. Ophthalmol. Vis. Sci. 51, 3660-3665.

Wang M., Ma W., Zhao L., Fariss R.N. and Wong W.T. (2011). Adaptive Müller cell responses to microglial activation mediate neuroprotection and coordinate inflammation in the retina. J. Neuroinflammation 8, 173.

Whitmire W., Al-Gayyar M.M., Abdelsaid M., Yousufzai B.K. and El-Remessy A.B. (2011). Alteration of growth factors and neuronal death in diabetic retinopathy: What we have learned so far. Mol. Vis. 17, 300-308.

Wässle H., Grünert U. and Röhrenbeck J. (1993). Immunocytochemical staining of aII-amacrine cells in the rat retina with antibodies against parvalbumin. J. Comp. Neurol. 332, 407-420.

Xiao M. and Hendrickson A. (2000). Spatial and temporal expression of short, long/medium, or both opsins in human fetal cones. J. Comp. Neurol. 425, 545-559.

Yamamoto H., Schmidt-Kastner R., Hamasaki D.I. and Parel J.M. (2006). Complex neurodegeneration in retina following moderate ischemia induced by bilateral common carotid artery occlusion in Wistar rats. Exp. Eye Res. 82, 767-779.

Accepted March 10, 2015